Injection Optimization for Heavy Duty Diesel Engine in Order to Find High Efficiency and Low NOx Engine Concept by Means of Quasi Dimensional Multi-Zone Spray Modeling

M. Keshavarz*
Development & Testing Manager
Iran Heavy Diesel MFG Co. (DESA)
Amol, Iran
m.keshavarz@desa.ir

G. Javadirad
PhD. Student
School of Mechanical Engineering
Nooshirvani University of Technology
g.javadirad@gmail.com

S. A. Jazayeri
Associate Professor
Department of Mechanical Engineering
K N Toosi University of Technology
g.javadirad@gmail.com

Corresponding Author*
Received: Feb. 18,2011
Accepted in revised form: May. 14,2011

Abstract

The purpose of this study is to investigate the effect of injection parameters on a heavy duty diesel engine performance and emission characteristics. In order to analyze the injection and spray characteristics of diesel fuel with employing high-pressure common-rail injection system, the injection characteristics such as injection delay, injection duration, injection rate, number of nozzle holes were investigated by using a quasi- dimensional model. In this work, different injection rate is considered with various injection parameters and performance and emission of the engine is simulated.

The aim of this work is finding the best injection system for a high efficiency and low NOx emission heavy duty diesel engine.

Keywords: *High efficiency, Low NOx, Multi-zone, diesel engine, spray modeling, Heavy duty*

1- Introduction:

Nowadays, heavy duty Diesel Engines are the main sources of electrical power generation and marine propulsion as well as electrical power generation required for rail traction. Similar to other combustion engines, these engines are the main sources of Green House gas and other pollutant emissions like NOx and PM.

The higher thermal efficiency of the engine is the most important key for the market economy and it could reduce the amount of Green House gasses. But higher thermal efficiency results in higher amount of NOx emission.

On the other hand, the environmental regulations against diesel engines are becoming tighter year after year and these engines require further development to meet future standards for gaseous and particulate exhaust emissions [1]. These legislations should be achieved in line with high efficiency engine in order to decrease life cycle cost and exhaust emitted CO_2 gas. Also, the reliability and durability of the engine should be held on acceptable level [2].

In order to produce smaller droplets and increase the efficiency of the engine, nozzle hole size should be reduced. Also, the injection pressure plays a significant role in both NOx emission and thermal efficiency of the engine.

In this study, multiple set of injector specification and injection strategies will be examined with common rail injection system to find the best configuration to achieve high efficiency and low NOx engine concept.

Multi-zone spray modeling is the efficient way to estimate DI diesel performance and emission and it is widely used in design and optimization of the engine. The good agreement of this model with experimental data made it a suitable way for studying the engine combustion characteristics.

Multi-Zone Spray Modeling

Multi-zone combustion model predicts the combustion rate and associated emissions for direct-injection diesel engines. This method was proposed by Hiroyasu[1] for the first time and sometimes it is called by his name.

The first step of this model, the initial Sauter mean diameter (SMD) of the fuel parcels is derived from fuel injection rate and the zone number. Then the air entrainment into each zone is considered as well as fuel vaporization and the fuel-air mixture will be constructed. Finally, ignition and combustion will be calculated from mixing and fuel evaporation rate.

The spray zones will be created in two directions: axial and radial. It means that liquid fuel is introduced into the domain by means of annular packages. Figure 1 shows the division of spray into zones at a certain time step.

It is assumed that there is no heat, mass and momentum transfer between the zones and that each annular section is subject to circumferential symmetry. The packages move forward so that they always remain in contact and cannot overtake one another.

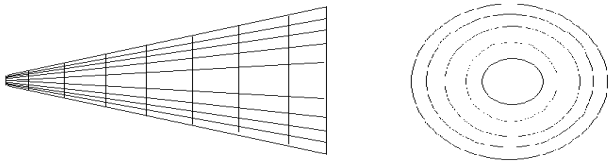

Fig 1. Schematic of the zone Structure

Individual zones experience their own history of temperature, pressure and composition. The total number of zones in the radial direction is fixed regardless of the amount of fuel injected or the time step used. The total number of zones in the axial direction is determined by the injection duration and the computational time step size [3].

2- Fuel injection Dynamics

The fuel injected into the cylinder is initially assumed to form a liquid column that travels at a speed equal to the fuel injection speed until the fuel break-up time elapses.

If it is assumed that the flow through each nozzle is quasi-steady, incompressible, and one dimensional, the mass flow rate of fuel injected through the nozzle is given by [4]:

$$\dot{m}_i = C_D A_n \sqrt{2\rho_L \Delta P} \qquad (1)$$

where

C_d is discharge coefficient

A_n is the geometrical nozzle area

ρ_l is the liquid fuel density

and ΔP is the pressure difference between cylinder and fuel inside injector.

The fuel injection velocity at the nozzle tip can be expressed as:

$$u_i = C_D \sqrt{\frac{2\Delta P}{\rho_L}} \qquad (2)$$

In the multi-zone model only the fuel spray is divided into a number of zones. The control volume of each zone is treated as an open system, and mass and energy equations are solved for each zone instead of solving the full momentum equation.

Spray penetration before and after breakup will be calculated from [3]:

$$\begin{cases} S = u_i t & 0 < t < t_b \\ S = 2.95\sqrt{\left(\frac{\Delta P}{\rho_a}\right)^{0.5} D \times t} & t_b \le t \end{cases} \quad (3)$$

where breakup time, tb, is:

$$t_b = 4.351\frac{\rho_l D}{C_D^2\sqrt{\rho_a \Delta P}} \quad (4)$$

Reitz and Bracco [5] proposed the following correlation for spray angle:

$$\theta = \tan^{-1}\left(\frac{4\pi\sqrt{3\frac{\rho_a}{\rho_l}}}{18 + 1.68\frac{L}{D}}\right) \quad (5)$$

The droplet size distribution within a zone, expressed in terms of the Sauter mean diameter is given by the following empirical expressions [6]:

$$SMD = MAX(SMD_{LS}; SMD_{HS}) \quad (6)$$

where

$$\begin{cases} \frac{SMD_{LS}}{D} = 4.12\,\mathrm{Re}^{0.12}\,We^{-0.75}\left(\frac{\mu_l}{\mu_a}\right)^{0.54}\left(\frac{\rho_l}{\rho_a}\right)^{0.18} \\ \frac{SMD_{HS}}{D} = 0.38\,\mathrm{Re}^{0.25}\,We^{-0.32}\left(\frac{\mu_l}{\mu_a}\right)^{0.37}\left(\frac{\rho_l}{\rho_a}\right)^{-0.47} \end{cases} \quad (7)$$

The number of drops in each zone can be determined knowing the SMD and the mass of fuel injected. Using an energy and mass balance for a single droplet in each zone, ordinary differential equations can be set up for the rate of change of the droplet temperature and diameter which is subsequently solved using a computational method. It will be explained more in the next section.

Air entrainment and Evaporation

The air entrainment rate into a given zone is controlled by the conservation of momentum applied to that zone. Therefore, the amount of entrained air of a zone is proportional to the decrement in the zone velocity:

$$\dot{m}_{ae} = -C_{ae} m_f u_i \frac{\frac{d^2 S}{dt^2}}{\left(\frac{dS}{dt}\right)^2} \quad (8)$$

In which Cae is the air entrainment factor. This factor should be selected from the experiments, and depends on engine speed, combustion chamber shape and injection specification.

Because of quiescent nature of flow in heavy duty diesel engines, the effect of swirl on spray deflection will be ignored.

With the assumption of uniform droplet temperature, the rate of droplet temperature change is determined by the energy balance equation, which states that the energy conducted to the droplet either heats up the droplet or supplies heat for vaporization. Therefore:

$$m_d c_{p,d} \frac{dT_d}{dt} = Q_{LV} \frac{dm_d}{dt} + q_{ht} \quad (9)$$

Convective heat transfer from the hot gas to liquid fuel droplets in a zone, q_{ht}, is modeled following the methodology which is simplified from the equation in reference 3.

$$q_{ht} = \pi d_d N k_m (T - T_d) Nu \quad (10)$$

where

N, is the number of droplets which is derived from the amount of fuel injected into a zone, initial SMD of each zone and density of the liquid fuel,

T, is the mean cylinder temperature,

km, is mean thermal conductivity which could be defined by the partial pressure of the fuel vapor and air and their conductivities.

The effects of boundary layer thickening due to mass transfer were not considered for simplicity in the above equation.

The rate of change in liquid droplet mass, $\frac{dm_d}{dt}$, is:

$$\frac{dm_d}{dt} = -\pi d_d N D_{va} Sh \frac{2P}{R_v(T + T_d)} \ln\left(\frac{P}{P - P_{v,s}}\right) \quad (11)$$

where

D_{va} , is the binary mass diffusivity between fuel vapor and air,

R_v , is the gas constant of the fuel vapor,

$P_{v,s}$, is saturation pressure of fuel vapor at temperature of T_d.

The Nusselt and Sherwood numbers are obtained from the following correlations [7]:

$$Nu = 2 + 0.6\,\mathrm{Re}_d^{0.5}\ \mathrm{Pr}^{0.33}$$
$$Sh = 2 + 0.6\,\mathrm{Re}_d^{0.5}\ Sc^{0.33} \qquad (12)$$

The Reynolds, Prandtl and Schmidt numbers are defined from the thermodynamic properties of the mixture of fuel vapor and air at mean temperature of air and droplet temperature.

The instantaneous mean diameter of droplets could be calculated from:

$$d_d = \left[\frac{6\left(m_{d,i} + \int dm_d\right)}{\pi N \rho_l}\right]^{0.33} \qquad (13)$$

3- Ignition delay and combustion

Ignition delay will be calculated from the following simplified Arrhenius equation [8]:

$$\tau_d = 2\times10^{-2}\,P^{-2.5}\varphi^{-1.04}\exp\left(\frac{4000}{T}\right) \qquad (14)$$

Ignition occurred when the following relationship is satisfied:

$$\int_0^{t_{ign}} \frac{dt}{\tau_{d,j}} = 1 \qquad (15)$$

The subscript j denotes that ignition starts when the above relationship is satisfied once in a zone. Therefore, the equivalence ratio should be calculated in each zone from the following expression:

$$\phi_j = \frac{m_{inj,j} - m_{d,j}}{f_{st} m_{a,j}} \qquad (16)$$

where

$m_{inj,j}$, is the total fuel injected into zone j,

$m_{d,j}$, is the instantaneous mass of liquid droplet in zone j,

f_s , is the stoichometric air-fuel ratio for the specified fuel,

$m_{a,j}$, is the instantaneous entrained air into zone j.

The model proposed by Hiroyasu [1] assumes that there is no single droplet surrounded by a flame and that the evaporated fuel reacts with the air entrained into the element forming a diffusion flame around a group of droplets.

This model assumes that combustion occurs at stoichometric conditions and that some residual portion of fuel or air in the element participates in the next step of combustion.

Therefore, the heat release rate for the jth zone can be written as:

$$\frac{dQ_j}{dt} = \begin{cases} LHV \times \dfrac{-dm_{d,j}}{dt} & \phi_j \le 1 \\ \dfrac{LHV}{f_{st}} \times \dfrac{dm_{ae,j}}{dt} & \phi_j > 1 \end{cases} \qquad (17)$$

Local temperature of each zone could be calculated from the 1st law of thermodynamics. Because it is assumed that there is no heat, mass and momentum transfer between the zones, the 1st law of thermodynamics could be expressed as:

$$m_i C_{p,i}\frac{dT_i}{dt} = -\dot{m}_{ae,j}h_a - m_{d,i}c_{p,d}\frac{dT_{d,i}}{dt} + \frac{(m_{ae,i} + m_{inj,i} - m_{d,i})}{\rho_m}\frac{dP}{dt} - \frac{dQ_j}{dt} \qquad (18)$$

The rate of pressure change in cylinder will be calculated from ideal gas law:

$$\frac{dP}{dt} = m\frac{d(RT/V)}{dt} \qquad (19)$$

The rate of change of the air zone temperature could be derived from 1st law of thermodynamics for air zone:

$$m_a C_p \frac{dT_a}{dt} = \sum_j \dot{m}_{ae,j}h_a - V_a + \frac{(m_{a,i} + m_{inj,i} - m_{d,i})}{\rho_m}\frac{dP}{dt} - q_{ht} \qquad (20)$$

where

qht, is heat transfer between walls and in cylinder gasses which is defined by Woschni[12] correlation and air zone temperature. The mean gas temperature will be calculated from:

$$T = \frac{m_a C_{p,a} T_a + \sum_j m_j C_{p,j} T_j}{m_a C_{p,a} + \sum_j m_j C_{p,j}} \qquad (21)$$

4- Nox & Soot Emission Modeling

The well-known extended Zeldovich mechanism is employed, which therefore only predicts the thermal contribution to NOx. Eleven chemical species are taken into consideration, namely: CO, CO_2, O_2, H_2, H_2O, OH, H, O, N and NO. Except for NO and N, all other species are assumed to be in thermodynamic equilibrium.

Soot is formed in the rich unburned-fuel-containing core of the fuel sprays and then is oxidized in the flame zone when it contacts unburned oxygen.

The soot formation rate is calculated by assuming a first-order reaction of vaporized fuel as proposed by Hiroyasu [9]:

$$\left(\frac{dm_{s,j}}{dt}\right)_F = A_f\left(m_{inj,j} - m_{d,j}\right)P^{0.5}e^{\left(\frac{-E_{sf}}{R_u T_j}\right)} \qquad (22)$$

$$E_{sf} = 1.25\times10^4\ kcal/mol$$

Where, Af, is constant that is determined by experimental data.

Soot oxidation model investigated in this study is the Nagle and Strickland-Constable [13] oxidation model. The NSC oxidation model is based on oxidation experiments of carbon graphite in an O_2 environment over a range of partial pressure. In this model, carbon oxidation occurs by two mechanisms whose rates oxidation occurs by two mechanisms [3]. The chemical reactions are:

$$\begin{aligned} &A + O_2 \leftrightarrow A + 2O \\ &B + O_2 \leftrightarrow A + 2O \\ &A \leftrightarrow B \end{aligned} \qquad (23)$$

The soot oxidation rate will be calculated from:

$$\left(\frac{dm_{s,j}}{dt}\right)_O = \frac{MW_C}{\rho_s d_s} m_{s,j} w \qquad (24)$$

Therefore,

$$\frac{dm_{s,j}}{dt} = \left(\frac{dm_{s,j}}{dt}\right)_F - \left(\frac{dm_{s,j}}{dt}\right)_O \qquad (25)$$

where

MW_C, is molecular weight of carbon,

ρ_s , is soot density (2.0 g/cm^3),

d_s , is soot diameter (4.5 x 10^{-9}m),

And w is net reaction rate of proposed reactions mentioned above.

This factor is calculated from the method mentioned in reference 3 and not presented here.

5- Model Validity

Because the target engine is new generation engine and it is under development in Iran Heavy Diesel Manufacturing CO. (DESA), we used another heavy duty diesel engine which is developed by MAN B&W named RK215. The specification of 16 cylinders RK215 which is tested in DESA and it is currently used in Iranian Railways, are listed in table 1. Table 2 and figure 2 show the differences between experimental data and simulation results.

Table 1. Specification of 16RK215 engine

Bore,mm	215	SOI,ATDCF	-20	Injection	Unit pump
stroke, mm	275	Speed,RPM	1000	Fuel per shot, mg	1226
con-rod length, mm	502	IVO	303.5	Ambient conditions	20 C, 1 bar
CR	13.5:1	IVC	-146.5	LT water temperature,C	68
Fuel	C13.5H27.6	EVO	121.5	Nozzle configuration	8 x 0.36
Type	DI-TC-IC	EVC	405.5	Injection duration,CA	30

Table 2. comparison between experimental and simulation results for 16RK215

Parameter	Simulation	Experimental
Brake power, kW	2840	2844
Maximum Cyl. Pressure, bar	156	154
Turbine inlet Temperature, C	607	555
T/C speed, RPM	24262	25740
Turbine outlet temperature, C	377	342
exhaust mass flow rate, kg/s	5.027	6.191
NOx concentration, ppm	914	1088

These results show good agreement between simulation and experimental data.

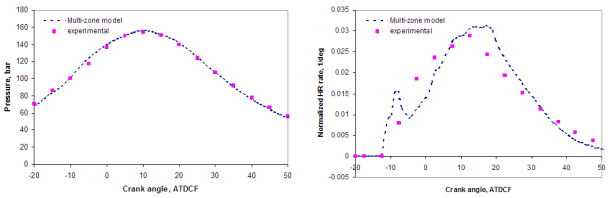

Fig 2. comparison between experimental and simulation cylinder pressure and calculated heat release

6- Development Targets

Because the high efficiency of the engine is one of the targets of this study, it needs to define the performance tar-

gets first. The major customer requirements in order of priority are reliability, availability, operating cost and ease of maintenance [10]. Another definition of thermal efficiency of the engine is brake specific fuel consumption, BSFC, which is defined as the amount of fuel delivered to the engine for the specified output power. This performance characteristic of the engine plays a major role in operating cost of the engine because the lower BSFC leads to lower operating cost. Also it is an important factor for the reliability of the engine, because the design requirement of the engine depends on its performance characteristics.

Figure 3 shows the scatter band of evolution in BSFC through the past years [11]. The future mean points are estimated and shown in this figure with dashed line.

As we know, the efficiency of internal combustion engines, like other thermal engines, is limited by the 2nd law of thermodynamics. The green band on figure 3 shows the minimum value of BSFC that could be reached by ideal diesel cycle in which no irreversibility is considered.

It should be noted that not only the 2nd law of thermodynamics limits the engine BSFC, but also the tight legislations on engine exhaust NOx emission makes designers ignore some improvements on the BSFC of their engines in order to decrease the NOx amount.

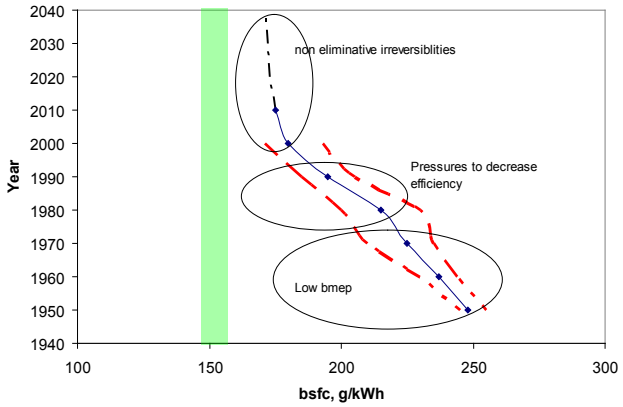

Fig 3. the evolution of BSFC of Heavy duty diesel engines through years

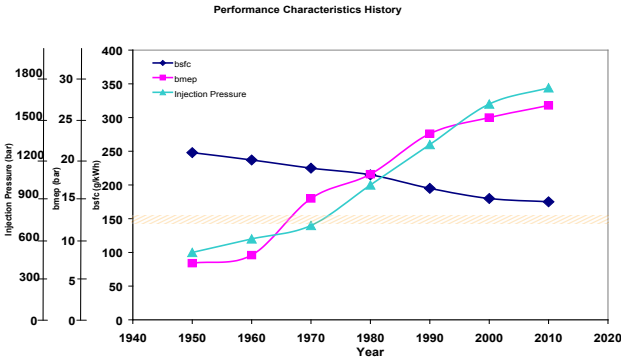

Fig 4. the history of performance characteristics of heavy duty diesels

Respect to figures 3 and 4, this BSFC target is a high efficient target and it needs some combustion requirements to achieve without exceeding the emission limits. But it should be noted that this value is overestimated (fewer than real target) in order to fill the gap between experimental and simulation data.

Also, as shown in figure 4, the injection pressure required to achieve the above targets should be as high as possible, so we decide to use high pressure common rail system for this engine.

7- Simulation Case definition

Figure 5, shows the injection pressure which is proposed by FIE supplier for configuration 1 (table 3) for the new engine. Also because of the characteristics of high pressure common rail system for large engines, a high order overshoot in injection pressure will be created as shown in figure 5.

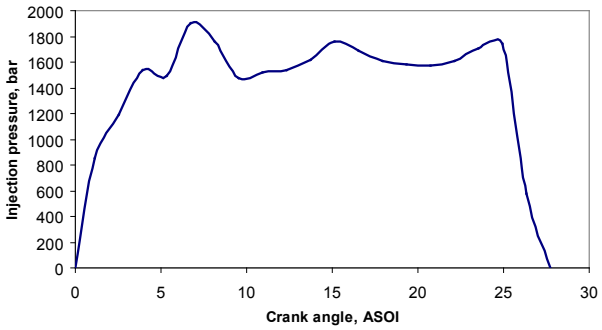

Fig 5. injection pressure for case 1 of table 3

The FIE supplier proposed 3 types of injectors with different number of holes and diameter. In the first matrix of injection configuration, different nozzle length respect to hole diameter has been considered. But the FIE supplier

asked us to keep the nozzle length as the fixed amount of 1.15mm for all of configurations. Also the injector cone angle was selected respect to injector/cylinder head design and optimized combustion chamber shape from the previous experiments of heavy duty diesel engines. The final shape of piston bowl has been optimized with CFD calculation later.

Also the injection strategies with multiple injections considered for the new engine. This strategy was defined with 5% and 10% pre-injection of diesel fuel. Figure 6 shows the injection pressure for case 3 of table 3 which is the case with pre-injection.

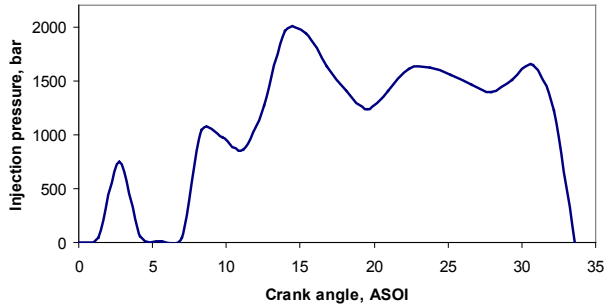

Fig 6. the injection pressure for case 3 of table 3

Table 3. Case definition for different nozzle configuration (370 mg/cycle fuel amount)

Case	Nozzle type	Injection Shape	Pilot Timing deg.ATDC	Pilot duration deg (ms)	Main Timing deg.ATDC	Main duration deg (ms)	Maximum Overshoot %
1	6 x 0.29	Standard	N/A	N/A	-7	26.37(2.93)	23.75%
2	6 x 0.29	5%P+ (2.5 dwell)	-12	2.3(0.256)	-6.25	24.8(2.756)	28.13%
3	6 x 0.29	5%P+ (5 dwell)	-13	2.3(0.256)	-4.75	24.8(2.756)	28.13%
4	6 x 0.29	5%P+ (5 dwell)	-12	2.3(0.256)	-3.75	24.8(2.756)	28.13%
5	6 x 0.29	10%P+ (2.5 dwell)	-12	3.75(0.42)	-5.8	24.1(2.68)	32.81%
6	6 x 0.29	10%P+ (5 dwell)	-13	3.75(0.42)	-4.3	24.1(2.68)	32.81%
7	6 x 0.29	10%P+ (5 dwell)	-12	3.75(0.42)	-3.3	24.1(2.68)	32.81%
8	7 x 0.27	Standard	N/A	N/A	-7	26.37(2.93)	23.75%
9	7 x 0.27	5%P+ (2.5 dwell)	-12	2.3(0.256)	-6.25	25(2.78)	31.56%
10	7 x 0.27	5%P+ (5 dwell)	-14	2.3(0.256)	-5.75	25(2.78)	31.56%
11	7 x 0.27	5%P+ (5 dwell)	-12	2.3(0.256)	-3.75	25(2.78)	31.56%
12	7 x 0.27	10%P+ (2.5 dwell)	-12	3.75(0.42)	-5.8	24(2.67)	32.81%
13	7 x 0.27	10%P+ (5 dwell)	-13	3.75(0.42)	-4.3	24(2.67)	32.81%
14	7 x 0.27	10%P+ (5 dwell)	-12	3.75(0.42)	-3.3	24(2.67)	32.81%
15	8 x 0.25	Standard	N/A	N/A	-7	25.14(2.79)	23.00%
16	8 x 0.25	5%P+ (2.5 dwell)	-12	2.3(0.256)	-6.35	23.9(2.656)	28.88%
17	8 x 0.25	5%P+ (5 dwell)	-14	2.3(0.256)	-6.8	23.9(2.656)	28.88%
18	8 x 0.25	5%P+ (5 dwell)	-12	2.3(0.256)	-4.8	23.9(2.656)	28.88%
19	8 x 0.25	10%P+ (2.5 dwell)	-12	3.84(0.426)	-6.25	23.5(2.722)	30.00%
20	8 x 0.25	10%P+ (5 dwell)	-14	3.84(0.426)	-5.25	23.5(2.722)	30.00%
21	8 x 0.25	10%P+ (5 dwell)	-12	3.84(0.426)	-3.25	23.5(2.722)	30.00%

The first simulation task is defined to find the best injection timing for each configuration. As shown in table 3, 21 configurations and strategy combinations were created, and then the simulation was started.

8- Simulation results

A: In-cylinder results

Firstly, two sets of in-cylinder results will be presented here: cases 1,3,6 for 6 holes injector and cases 15,17, 20 for 8 holes injector.

Figure 7 shows the liquid fuel mass in cylinder for set 1 and 2 of the results.

This figure shows that the major advantage of pre-injection is decreasing in the amount of fuel-air mixture just before the start of combustion. This issue makes the mixture formation to be step by step during injection hence it avoids the large premix heat release at the first phase of combustion. Also pre-injection would cause the injection to start earlier than standard type for an

Because mixing before start of combustion in set2 is better than set 1, more premix combustion will happen in set 2. This improvement in mixing air and fuel results from improvement in discharge coefficient as well as shortening injection duration in order to deliver the same amount of fuel. It is expected that the NOx amount in set 2 of results will be more than their set 1.

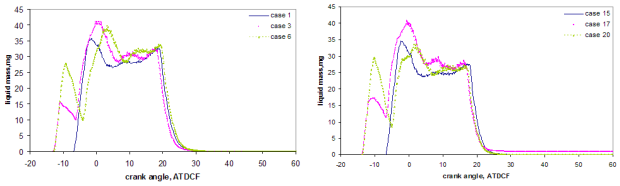

Fig 7. in-cylinder liquid fuel mass VS time

Figure 9 shows the cylinder pressure diagram for set 1 and 2 of results. As shown in these diagrams, pre-injection could eliminate the high rate of pressure rise due to premix combustion.

Also cylinder temperature for set 1 and 2 of results is shown in figure 10. As shown in these diagrams, the maximum temperature of the cylinder with 8 holes injector has not the same trend (pre-injection VS standard type) as 6

holes type. This should be resulted from different start of injection for pre-injection type in these two types of injectors. But the maximum cylinder temperature with set 2 is higher than set 1 while the location of maximum temperature is nearly the same. This issue results in higher NOx amount in 8 holes nozzle configuration.

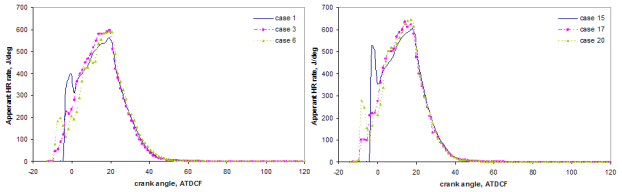

Fig 8. apparent heat release rate VS time

Figure 11 shows the in-cylinder NOx amount versus crank angle. These diagrams show that the NOx amount in the cylinder for set 1 of results will decrease with pre-injection because the high rate of premixed combustion has been eliminated and the maximum temperature has been decreased in the same crank angle.

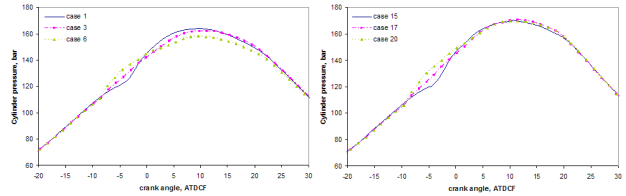

Fig 9. in-cylinder pressure VS crank angle

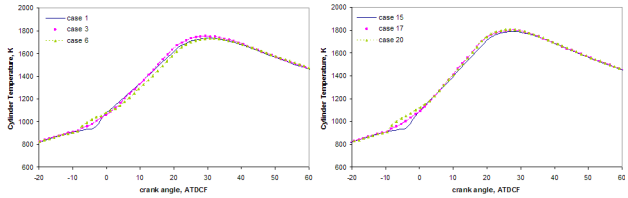

Fig 10. in-cylinder temperature VS crank angle

In set 2 of results, the NOx amount is higher than set 1; this is because of shorter injection duration due to decrease of nozzle hole diameter.

Figure 12 also show the soot concentration in semi logarithmic diagram.

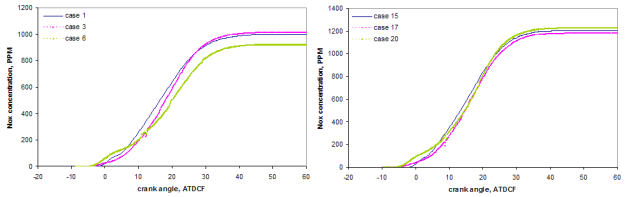

Fig 11. in-cylinder NOx amount VS crank angle

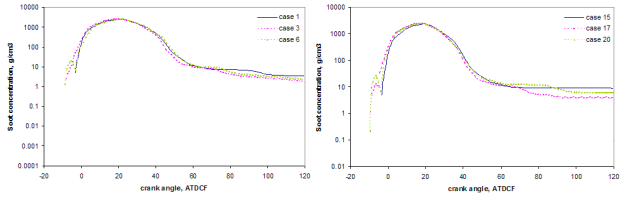

Fig 12. in-cylinder soot concentration VS crank angle

B: Engine performance results

Table 4 shows the engine performance and emission results for all 21 simulation cases. In order to find better injection parameters to reach better engine performance and emission, some scatter diagrams are provided. Figure 13 shows the BSFC scatter band with different maximum overshoot. The pink band shows the range of overshoot in which BSFC of 199 g/kWh could be achieved without any significant retarding of main injection timing.

The simultaneous increase in amount of NOx and Soot, in some cases is due to using Pre-injection system which decreases the rate of premixed combustion and NOx amount. Depending on the extent of NOx reduction, an earlier injection and combustion start is possible, resulting in an increase in thermal efficiency.

Figure 14 shows the maximum overshoot with overall injection duration (pre + main without considering dwell time). The previous pink band is transposed to this diagram.

But if the duration of injection in standard cases revised, they could be used to achieve BSFC of 199 g/kWh without any significant retarding of standard injection.

Figure 15 shows the scatter band of BSFC in terms of dwell time. It is clear that dwell time between 3 and 5 is good, the 4 degree is the best, but it depends on the start of main injection.

Finally figure 16 shows the scatter diagram of BSFC in terms of start of main injection. This figure explains why we are not going to retard the main injection timing any further. This figure shows that for the BSFC target of 199

g/kWh, the main injection timing should be located between -6 and -2.5 ATDCF.

At last, Figure 17 shows the BSFC and NOx trade-off and target point. This trend shows that for BSFC=199 g/kWh slightly lower than 9 amount of NOx could be achieved. This figure also shows that the cases 10 and 13are the best two cases which are within the performance and emission targets.

Table 4. performance and emission results

Case	Nozzle type	Injection Shape	BSFC g/kWh	BsNOx g/kWh	BsSOOT g/kWh	Pmax bar
1	6 x 0.29	Standard	197.87	9.37	0.01703	163.99
2	6 x 0.29	5%P+ (2.5 dwell)	197.64	9.53	0.01832	162.59
3	6 x 0.29	5%P+ (5 dwell)	197.73	9.41	0.01793	162.26
4	6 x 0.29	5%P+ (5 dwell)	200	8.12	0.01625	153.95
5	6 x 0.29	10%P+ (2.5 dwell)	197.55	9.75	0.0182	165.25
6	6 x 0.29	10%P+ (5 dwell)	199.35	8.68	0.01623	158.5
7	6 x 0.29	10%P+ (5 dwell)	200.5	8.1	0.01659	154.7
8	7 x 0.27	Standard	197.61	9.47	0.01616	164.23
9	7 x 0.27	5%P+ (2.5 dwell)	198	9.25	0.01723	162.93
10	7 x 0.27	5%P+ (5 dwell)	198.5	8.98	0.01579	160.25
11	7 x 0.27	5%P+ (5 dwell)	201.4	7.33	0.01430	152.43
12	7 x 0.27	10%P+ (2.5 dwell)	197.28	9.85	0.01268	165.6
13	7 x 0.27	10%P+ (5 dwell)	199.03	8.76	0.01392	159
14	7 x 0.27	10%P+ (5 dwell)	200.15	8.145	0.01435	155.01
15	8 x 0.25	Standard	195.44	11	0.0426509	169.7
16	8 x 0.25	5%P+ (2.5 dwell)	195.52	11.23	0.0445	168.7
17	8 x 0.25	5%P+ (5 dwell)	196.05	10.74	0.0425	170.5
18	8 x 0.25	5%P+ (5 dwell)	198.05	9.18	0.05042	160.95
19	8 x 0.25	10%P+ (2.5 dwell)	194.97	12.09	0.04239	175.4
20	8 x 0.25	10%P+ (5 dwell)	195.88	11.1	0.048483	170
21	8 x 0.25	10%P+ (5 dwell)	197.48	9.69	0.04992	161.06

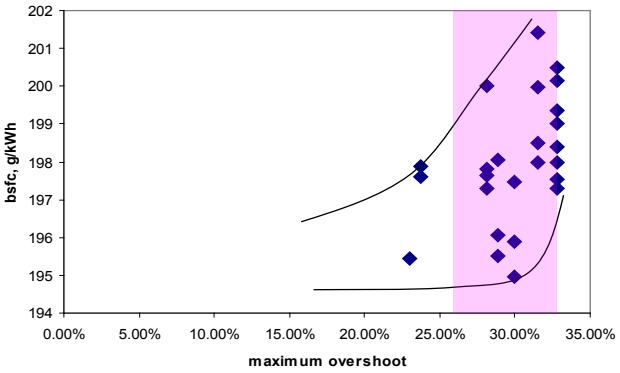

Fig 13. BSFC scatter band with different maximum overshoot

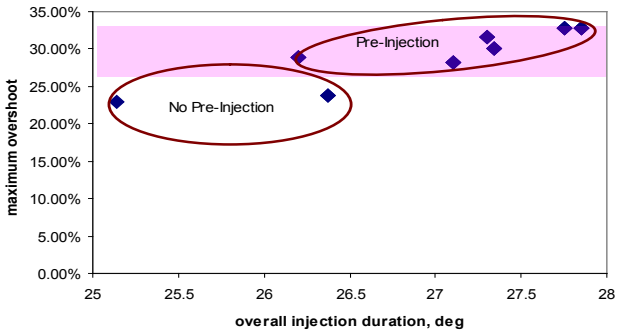

Fig 14. maximum overshoot VS overall injection duration

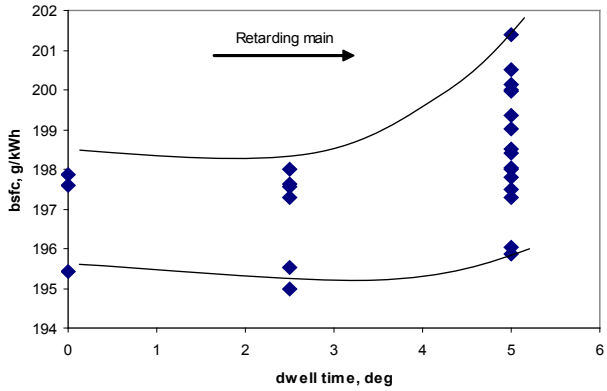

Fig 15. scatter band of BSFC in terms of dwell time

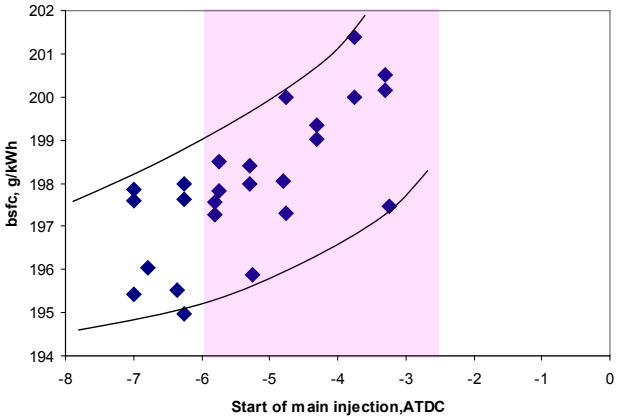

Fig 16. scatter diagram of BSFC in terms of start of main injection

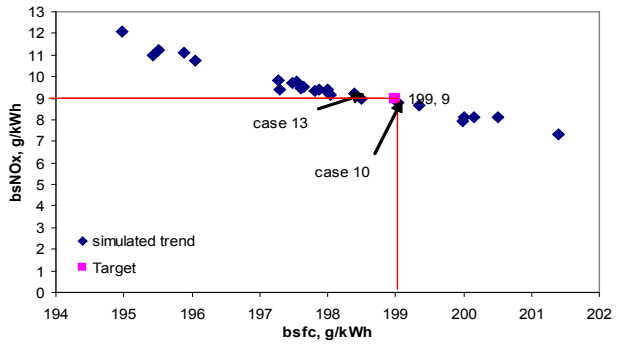

Fig 17. BSFC and NOx trade-off with recommended points

Conclusions

The results could be summarized as follows:

- The results of multi-zone model have a good agreement with experiment and could be used in new engine development process with acceptable level of reliability and confidence.
- The major advantage of pre-injection is reducing of the amount of fuel-air mixture just before start of combustion. This issue makes the mixture formation to be done step by step during injection; therefore it avoids the large premix heat release at the first phase of combustion.
- The soot concentration will be decreased dramatically with pre-injection.
- The targets for BSFC and NOx amount in order to have the high efficiency and low NOx engine concept could be achieved using pre-injection without retarding main injection timing and increasing of smoke amount.
- It is suggested that in order to find better results for optimum points, the multi objective optimization will be carried out with generic algorithm.

References:

[1]- J. Hlousek, M. Bernhaupt,B Kogler ,"Electronically controlled injection rate shaping for medium speed diesel engines",23th CIMAC Congress,2001, Hamburg

[2]- J. Hlousek, " Common rail system for large diesel engines", Paper no 117, 24th CIMAC Congress,2004, Kyoto

[3]- D. Jung, D. Assanis, "Multi-Zone DI Diesel Spray Combustion Model for Cycle Simulation Studies of Engine Performance and Emissions", SAE paper No. 2001-01-1246

[4]- J. B. Heywood, " Internal combustion engines fundamentals",3rd edition, McGraw Hill, 1988

[5]- Reitz, R. D. and Bracco, F. B., "On the Dependence of Spray Angle and Other Spray Parameters on Nozzle Design and Operating Conditions," SAE Paper 790494

[6]- Hiroyasu, H., Arai, M., and Tabata, M., "Empirical Equations for the Sauter Mean Diameter of a Diesel Spray," SAE Paper 890464, 1989.

[7]- W. E. Ranz, W. R. Marshall,"Evaporation from drops.", Chem. Eng. Prog., Vol. 48, No. 4, 1952

[8]- J. I. Ramos, " Internal combustion engine modeling", Hemisphere publishing corporation, 1989

[9]- Hiroyasu, H., Kadota, T. and Arai, M., "Development and Use of a Spray Combustion Modeling to Predict Diesel Engine Efficiency and Pollutant Emissions (part 1: Combustion Modeling)", Bulletin of the JSME, Vol. 26, No. 214,1983

[10]- F. Starke, U. Hopmann, "Caterpillars electronically controlled injection systems for Medium Speed Engines", Paper no 188, 25th CIMAC Congress,2007, Vienna

[11]- Wartsilae Corporation, "VASA22 engine technical documents", Technical Archive of Iran Heavy Diesel Engine MFG Co.

[12]- Woschni G, "A Universally Applicable Equation for the instantaneous Heat Transfer Coefficient in the Internal Combustion Engine", SAE Transactions, Vol. 76, p. 3065, 1967

[13]- Nagle, J. and Strickland-Constable, R.F., "Oxidation of Carbon Between 1000-2000 C" Proc. 5th Conf. on Carbon, vol. 1, Pergamon Press, 1962, p. 154.